Drop Size Distribution and Holdup Profiles in a Multistage Extraction Column

C. Tsouris, V. I. Kirou, and L. L. Tavlarides
Dept. of Chemical Engineering and Materials Science, Syracuse University, Syracuse, NY 13244

A population-balance-equation model is employed for the analysis of liquid-liquid extraction columns. This model considers drop breakage, coalescence, and exit phenomena for the drop phase caused by drop-drop and drop-continuous phase interactions. Drop breakage and coalescence rates are employed from a previous study on liquid dispersions in stirred-tank contactors. A drop exit frequency is developed based on a stochastic modeling approach. The model is tested by drop size distribution and dispersed-phase volume fraction (holdup) data obtained for a multistage column contactor of pilot-plant scale. Steady-state drop size distribution and transient holdup measurements are obtained by a photomicrographic technique and an ultrasonic technique, respectively. The model can predict flooding of the column. The effect of mass transfer on the hydrodynamic parameters of the contactor is also examined. The population-balance-equation model can be used for the control of extraction columns and can be extended to include mass-transfer calculations for the prediction of extraction efficiency.

Introduction

Liquid-Liquid extraction is one of the classical methods in separation technology and finds applications in the chemical and petroleum industry, hydrometallurgy, biotechnology, nuclear technology, waste management, and other areas. The objective of this process is the separation of the components of a homogeneous liquid solution by using another solvent or a reactive liquid solution. The two liquid systems are immiscible or partially miscible and are introduced into contacting equipment where a liquid dispersion with high enough interfacial area for mass transfer is created by agitation. Extraction columns are one type of contacting equipment which are divided into several categories depending upon the geometry and the method in which mixing is provided to the liquid dispersion. The hydrodynamic and mass-transfer behavior of one such column contactor, the multistage stirred-cell extraction column (known also as MIXCO or Oldshue-Rushton column, as shown in Figure 1), is investigated in this study. The modeling approach, however, is not limited to the specific type of equipment. In fact, similar modeling has already been applied in studies of other types of extraction columns.

Current approaches for the design of extraction columns do not consider the nonhomogeneous character of the dispersed phase and the individual properties of the drops which depend on the drop size. Such properties are the residence time and the rate of mass transfer. Although the current design strategies have been successful to date, a better understanding of the process is required for the optimization of equipment performance and reduction of the number of tests in the scaleup process.

A more detailed approach for the analysis of the extraction process in column contactors has been pursued by Jiricny et al. (1979a,b), Cruz-Pinto and Korchinsky (1981), Sovova (1983), Laso et al. (1984), Casamatta and Vogelpohl (1985), and others. This approach is based on the population balance equation (Hulburt and Katz, 1964; Randolph and Larson, 1966; Ramkrishna, 1985) and considers drop breakage, coalescence, and exit rates. Nonuniform holdup profiles and drop size distributions along the contactor have been explained by this type of modeling. The convective nature of the drops is recognized by this approach. Also, this approach permits stud-

Correspondence concerning this article should be addressed to L. L. Tavlarides.
C. Tsouris is currently with the Chemical Technology Div., Oak Ridge National Laboratory, P.O. Box 2008, Oak Ridge, TN 37831.
V. I. Kirou is currently with A. Hatzopoulos S.A., Flexible Packaging for Food Stuffs, Thessaloniki, Greece 54628.

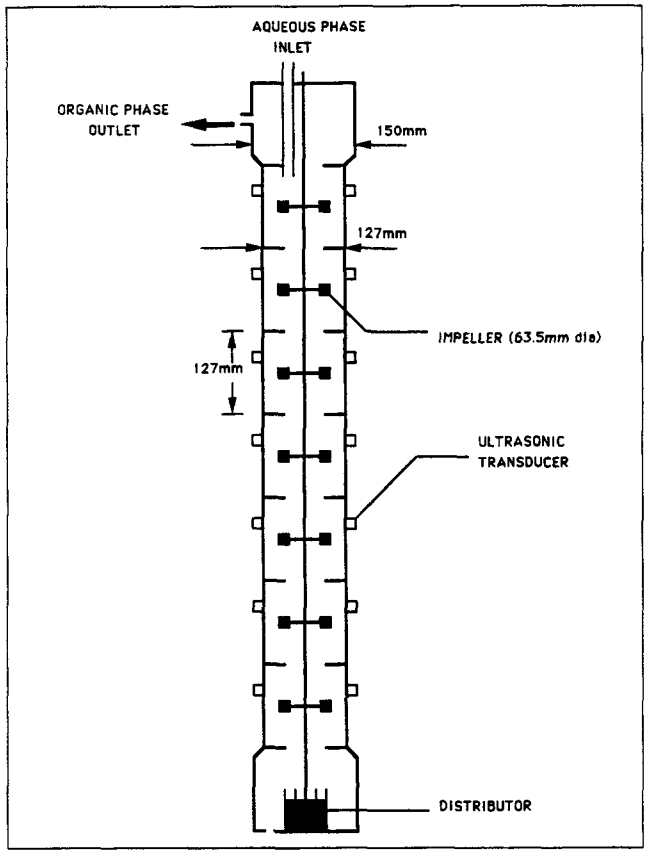

Figure 1. Multistage stirred-cell column contactor.

ies of the effect of drop-drop and drop-continuous phase interactions on drop size and holdup. The drop size and holdup determine the interfacial area for mass transfer and are, therefore, needed for equipment design. Currently, these parameters are provided by empirical correlations.

Although the population balance equation can accommodate multiple drop properties, such as size, concentration, age, and residence time, the solution of the equation becomes complicated even for the consideration of only two of the above properties. Therefore, stochastic simulation techniques have been introduced (Spielman and Levenspiel, 1965; Zeitlin and Tavlarides, 1972; Shah et al., 1977; Hsia and Tavlarides, 1980, 1983; Bapat et al., 1983; Bapat and Tavlarides, 1985; Guimaraes et al., 1990; Kirou, 1990; Kirou and Tavlarides, 1994) to overcome the complexity of the differential equations. From the above references, only the work of Kirou and Tavlarides (1994) pertains to extraction columns. All the other studies have been performed for stirred tank contactors. In order to represent a multistage extraction column, Kirou and Tavlarides (1994) extended an event-oriented simulation of a stirred-tank contactor to account for interconnected multiple stages. As such, the approach describes dispersed phase holdup and drop size distribution profiles along the contactor. Extensions are readily made to accommodate mass transfer for the prediction of the extraction efficiency of the column. A significant disadvantage of this approach, however, is that it requires extensive computational time.

In the present study, a population-balance-equation model is developed to predict the drop size distribution and holdup profiles in a multistage stirred-cell contactor. The model is tested against experimental data. The advantage of this model over stochastic simulation techniques is that it requires much less computational time, smaller than the process time constant, which permits use of model-based predictive control strategies. The model can also be extended to accommodate mass transfer.

Model Development

Population balance equation

The population balance equation (Hulburt and Katz, 1964; Randolph and Larson, 1966; Ramkrishna, 1985) has proved to be an extremely useful tool for the modeling of liquid dispersions due to its ability to describe both continuous processes such as mass transfer and chemical reactions and abrupt changes such as drop breakage and coalescence.

To employ the population balance modeling approach, the multistage column contactor is represented by a series of interconnected stirred tanks with forward and backward flow components for both phases. A population balance equation is written for each cell. The equation accounts for drop birth (B) and death (D) terms due to breakage and coalescence and other appropriate terms to describe drop convection between consecutive cells. The convective terms are introduced in the form of exit frequency functions. The population balance equation for the drop size distribution in the ith cell of the column contactor is written as:

$$\frac{dn^i(v,t)}{dt} = n^{i-1}(v,t)Z_{e,f}^{i-1}(v,t) - n^{i+1}(v,t)Z_{e,b}^{i+1}(v,t) - n^i(v,t)[Z_{e,f}^i(v,t) + Z_{e,b}^i(v,t)] - D^i + B^i \quad (1)$$

where $n^i(v,t)$ is the number of drops in the ith stage of volume v at time t, and $Z_{e,f}$ and $Z_{e,b}$ are the forward and backward exit frequencies, respectively. The term on the lefthand side of the equation represents the accumulation of drops, the first two terms on the righthand side represent input of drops from the adjoining cells, the next term represents output of drops to adjoining cells, and, D^i and B^i are the terms representing the death and birth of drops and are given by the following relations:

$$D^i = n^i(v,t)\int_0^\infty \lambda(v,v')h(v,v')n^i(v',t)dv' + g(v)n^i(v,t) \quad (2)$$

$$B^i = \int_0^{v/2} \lambda(v-v',v')h(v-v',v')n^i(v-v',t)n^i(v',t)dv' + \int_v^\infty \beta(v',v)\nu(v')g(v')n^i(v')dv'. \quad (3)$$

In Eqs. 2 and 3, $g(v)$ represents the drop breakage rate, $\nu(v)$ is the number of daughter drops produced by breakup of a drop of volume v ($\nu=2$ for binary breakup), $\beta(v', v)$ is the drop probability density of daughter drops formed by breakup of drops of volume v', $h(v', v)$ is the collision frequency of drops of volume v and v' and $\lambda(v', v)$ is the coalescence efficiency.

Drop frequency functions

The drop frequency functions of breakage and coalescence needed for the solution of Eq. 1 are assumed to be identical to the ones developed in the first part of this work for the analysis of a batch stirred-tank contactor (Tsouris and Tavlarides, 1994). This assumption is reasonable because of geometric similarities between the stirred tank contactor and each of the cells of the multistage stirred-cell extraction column which is being modeled. The only differences are the volume of each of the column cells is twice the volume of the tank, and the column cells are interconnected, whereas the tank is a closed system. The only unknown required for the solution of Eq. 1 is the exit frequency function which connects the individual cells of the column contactor. The development of this frequency is presented in the next section.

Drop exit frequency

The drop exit frequency proposed here is an extension of the model proposed by Kirou (1990) and attempts to represent the effects of interstage flows on drop convection from one stage to another. According to this model, the drop exit frequency is given by:

$$Z_e(d) = F_{exp} \cdot P_{exit} \cdot P_{loop}. \tag{4}$$

Here, F_{exp} is the frequency of exposure in the critical layer between two consecutive cells, P_{exit} is the conditional probability of exit from one cell to the next given that the drop is in the critical layer, and P_{loop} is the probability that a drop will be in the circulation loop. It should be clarified here that consecutive cells in the investigated multistage column are separated by horizontal plates with annular openings in the center, and that the critical layer is assumed to be a film of a certain width covering the free area in the annular openings in the horizontal plates between consecutive cells. The exit frequency model assumes that the frequency of exposure in the critical layer is equal to the circulation frequency which is obtained from a correlation by Holmes et al. (1964) as:

$$F_{exp} = F_{circ} = t_{circ}^{-1} = \left[0.85 \frac{1}{rps} \left(\frac{D_T}{D_i} \right)^2 \right]^{-1}. \tag{5}$$

In the above relation, t_{circ} is the average circulation time of the continuous phase, rps is the agitation speed, and D_T and D_i are the tank and impeller diameters, respectively.

For the probability, P_{loop}, it is assumed that a drop has equal probability to be found anywhere in the cell. This assumption neglects the buoyancy effect. It is also assumed that the loop consists of two cylindrical jets, one in the upper part of the cell, as shown in Figure 2, and one in the lower part. The thickness of each jet is taken as half of the width of the impeller blade. Then, the probability, P_{loop}, is obtained by the following relation:

$$P_{loop} = \frac{V_{loop}}{V_T} = \frac{\pi \left(\frac{D_i}{2} - \delta \right) \delta \left(\pi \frac{D_i}{2} \right)}{V_T} \tag{6}$$

where V_{loop}, V_T are the volumes of the loop and cell, respectively, and δ is the critical region or jet thickness taken as half the width of the impeller blade.

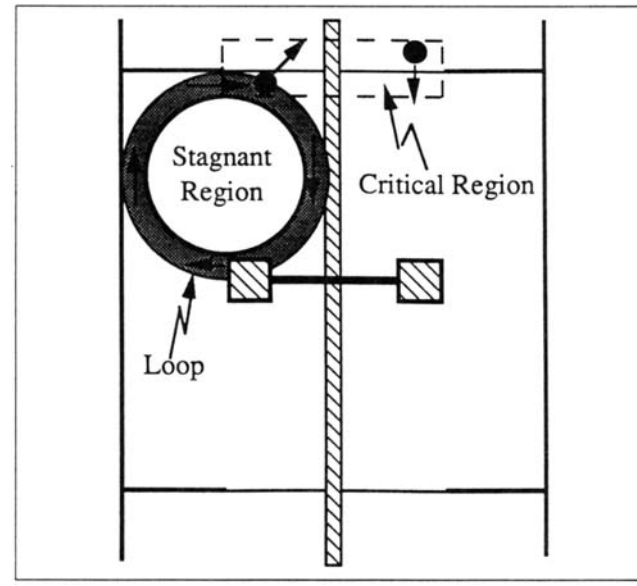

Figure 2. Circulation loop in a stirred-cell contactor.

A drop will exit a stage once in the critical region (see Figure 2) if the penetration time of the drop through the critical region, t_p, is smaller than the exposure time of the drop in the critical region, t_e. The conditional probability function P_{exit} can now be written for the drops in this region as:

$$P_{exit} = P\{ (t_p, t_e) : t_p < t_e) \} \tag{7}$$

The probabilistic approach described above, where one has to identify characteristic times and calculate the probability of interest as a subset of the sample space, has been used by several authors to express the probabilities for drop breakup and coalescence (for example, Ross, 1971; Coulaloglou and Tavlarides, 1977).

To evaluate P_{exit}, the probability distributions of the exposure time and of the penetration time are needed. Both the exposure and penetration time are considered random variables. There are no experimental data for either of these times and, therefore, adoption of some models will be required. First, the exposure time is modeled as follows. Suppose a drop has entered the critical region. The time it takes for the drop to exit the region in any possible way is a nonnegative number, that is, the sample space is $\Omega = (0, \infty)$. One can further assume that if the drop has stayed in the region up to time t, its probability to exit between time t and $t + \Delta t$ depends only on Δt. This means that (a) the time of exposure is a "memoryless" random variable, and (b) the probability of exiting from the region can be expressed by a linear relation in Δt. It should be explained here that a random variable X is said to be "memoryless" (Ross, 1980) if $P\{X > s + t | X > t\} = P\{X > s\}$ for all $s, t \geq 0$. Also, the linearity we are referring to, typical of a Poisson process, can be expressed as: $P\{\text{exit}(t, t+h) | \text{ stayed until } t\} = \lambda h + o(h)$ as $h \downarrow o$, λ being a positive constant.

Assumptions a and b lead to the exponential distribution (Ross, 1980):

$$P(t_e)=\frac{1}{\bar{t}_e}\exp\left[-\frac{t_e}{\bar{t}_e}\right]. \tag{8}$$

Using this form, we redefine $\bar{t}_e$ here as:

$$\bar{t}_e=\frac{r_e}{u_r} \tag{9}$$

where

$$r_e=r_f-r', \tag{10}$$

r_f is the radius of the free circular area between two consecutive cells, and r' is the diameter of a restricted circular area. The restricted area is considered to account for local flow patterns between consecutive stages created by the impellers. u_r is the radial velocity of the continuous phase in the critical layer and is given by Ju et al. (1990) as:

$$u_r=0.1u_{\text{tip}}=0.1\pi ND_i \tag{11}$$

where N is the agitation speed. For the local axial velocity, a linear profile is considered, as shown in Figure 3. It should be mentioned here that the impellers used in this work receive fluid axially and discharge radially. The linear profile can be described by the following relation:

$$U_Z=\left(1-\frac{r}{r_c}\right)U_{\max} \quad \text{for } 0<r<r_c \tag{12}$$

and

$$U_Z=0 \quad \text{for } r_c<r<r_f. \tag{13}$$

$U_{\max}$ is assumed to be proportional to the impeller tip velocity:

$$U_{\max}=K_1\pi D_i N \tag{14}$$

where the proportionality constant, $K_1=0.2$ according to Ju et al. (1990). Also, r_c is assumed to be proportional to r_f:

$$r_c=\frac{N}{N_f}r_f \tag{15}$$

which implies that

$$r_c=r_f \quad \text{for } N=N_f$$

and

$$r_c=0 \quad \text{for } N=0. \tag{16}$$

N_f is, therefore, the agitation speed at which $r_c=r_f$. From the above considerations, the axial velocity profile in the critical layer becomes:

$$U_Z=\left(1-\frac{r}{\frac{N}{N_f}r_f}\right)U_{\max}. \tag{17}$$

The local velocity profile is superimposed on the continuous-phase velocity which has direction from top to bottom, as shown in Figure 4. The top diagram shows the local velocity profiles in the critical layer due to agitation and without continuous-phase net flow. The diagram in the middle shows the velocity profile for the stage above, (δ^+), while the bottom diagram shows the velocity profile for the stage below, (δ^-), for nonzero continuous-phase flow. Mass interchange due to velocity fluctuations is considered to be the same in all directions, and therefore, only the net flow is considered here. The following condition has to be satisfied for the net flow rate of the continuous phase at δ^+:

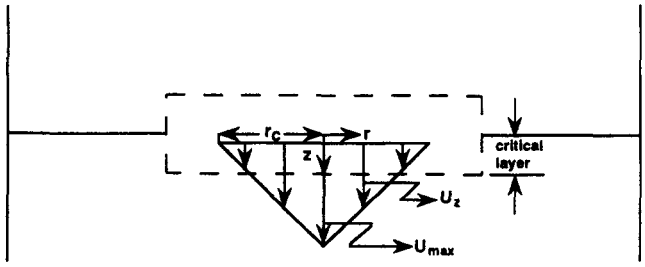

Figure 3. Local axial velocity profile between consecutive cells due to agitation.

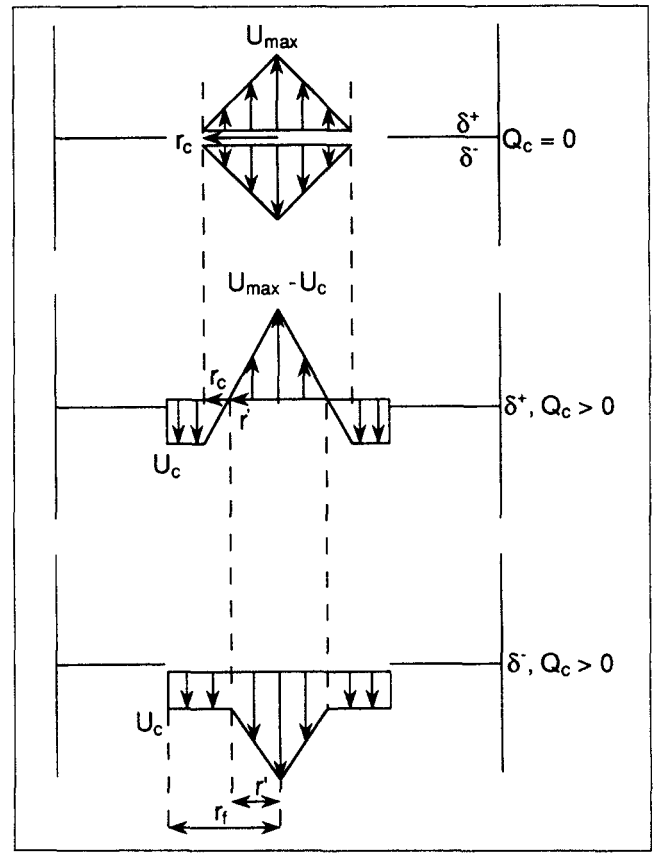

Figure 4. Velocity profiles with and without countercurrent flow.

$$Q_c = \int_{r'}^{r_c} \left\{ U_c - \left(1 - \frac{r}{r_c}\right) k_1 \pi D_i N \right\} 2\pi r dr + \int_{r_c}^{r_f} 2\pi r U_c dr \quad (18)$$

where r' is the distance from the center of the free area between the cells at which the velocity profile in the above stage crosses the zero line, and U_c is the continuous-phase velocity between r' and r_f. Also, from geometric considerations, one can write:

$$\frac{U_c}{U_{\max} - U_c} = \frac{r_c - r'}{r'} \quad (19)$$

or

$$U_c = \frac{r_c - r'}{r_c} U_{\max} = \left(1 - \frac{r'}{r_c}\right) k_1 \pi D_i N. \quad (20)$$

Substituting Eq. 20 in Eq. 18, integrating and rearranging terms, one obtains:

$$\frac{Q_c}{\pi^2 k_1 D_i N} - \left(1 - \frac{N^2}{3N_f^2}\right) r_f^2 + \frac{N_f}{N} r' r_f - \frac{N_f}{3N} \frac{r'^3}{r_f} = 0. \quad (21)$$

This equation can be solved by the Newton method for a given value of the parameter N_f to provide r' which can be used in Eq. 20 for the calculation of U_c. Also, the calculated value of r' is used in Eq. 10 to determine r_e. The assumption made by Eq. 10 is that drops in the critical layer can move to the above cell only through the area between r' and r_f. This assumption recognizes that the resistance due to the countercurrent flow of the continuous phase is minimum between r' and r_f. From Eqs. 9, 10, 11 and 20, one can estimate the mean exposure time and the net velocity of the continuous phase.

The penetration time can be estimated by the following relation (Kirou, 1990):

$$t_p = \frac{\delta}{u(d)} \quad (22)$$

where $u(d)$ is the instantaneous drop velocity and is estimated as the summation of the drop velocity in a stagnant medium and a drop velocity component due to the continuous phase flow. Accordingly, $u(d)$ is given as:

$$u(d) = u_d(d) + u_c. \quad (23)$$

Here, u_c is a continuous-phase velocity component which is given below, and u_d is the terminal velocity of a drop rising in a stagnant medium which is obtained by Klee and Treybal (1956) as:

$$u_d(d) = 38.3 \rho_c^{-0.45} \Delta\rho^{0.58} \mu_c^{-0.11} d^{0.70}. \quad (24)$$

where ρ_c and $\Delta\rho$ are in g/cm^3, μ_c is in g/cm·s, and d is in cm. Kirou (1990) assumed a normal distribution for u_c and obtained the following probability density function:

$$P(t_p) = \frac{\delta}{t_p^2 \sigma^* \sqrt{2\pi}} \exp\left[-\frac{1}{2} \left(\frac{\delta/t_p - u_d - \mu^*}{\sigma^*} \right)^2 \right] \quad (25)$$

where μ^* and σ^* are the mean and standard deviation of the distribution. The values of these parameters are obtained as follows: u_c is decomposed into an average and a fluctuation component, u_z:

$$u_c = -\frac{U_c}{1-\phi} + u_z \quad (26)$$

where $-U_c/(1-\phi)$ is the mean μ^* of the distribution given by Eq. 25. The standard deviation of the distribution is taken to be the root-mean-square value of the fluctuation component of the velocity which can be estimated by the following relation due to Schwartzberg and Treybal (1968):

$$\sigma^* = u_z' = \sqrt{u_z^2} \approx 0.462 \frac{(rps) D_i^2}{(H D_T^2)^{1/3}}. \quad (27)$$

H, D_T are the height and diameter of the tank, respectively. The above relation has been obtained by analysis of velocity measurements in a stirred tank.

From Eqs. 7, 8, and 25, one can express the drop exit probability by the following integral (Kirou, 1990):

$$P_{\text{exit}} = \int_0^\infty \lambda \exp(-\lambda x) \left[\int_{y=0}^{y=x} P(y) dy \right] dx \quad (28)$$

where $P(y)$ is given by Eq. 25, and $\lambda = 1/\bar{t}_e$. It can be shown (Kirou, 1990) that the probability of forward exit is given by:

$$P_{\text{exit},f} = \frac{\delta}{\sigma^* \sqrt{2\pi}} \int_0^\infty \frac{1}{x^2} \exp(-\lambda x) \times \exp\left\{ -\frac{1}{2\sigma^{*2}} \left[\frac{\delta}{x} - \left(u_d - \frac{U_c}{1-\phi} \right) \right]^2 \right\} dx. \quad (29)$$

Also, the probability of backward exit is given by:

$$P_{\text{exit},b} = \frac{\delta}{\sigma^* \sqrt{2\pi}} \int_0^\infty \frac{1}{x^2} \exp(-\lambda x) \times \exp\left\{ -\frac{1}{2\sigma^{*2}} \left[\frac{\delta}{x} + \left(u_d - \frac{U_c}{1-\phi} \right) \right]^2 \right\} dx. \quad (30)$$

Hence, the drop forward and backward exit frequency functions are given from Eqs. 4, 5, 6, 29 and 30. The only parameter in these functions is the agitation speed, N_f, at which $r_c = r_f$. The value of this parameter has been obtained by fitting results of holdup and drop size from the solution of the population balance equation to experimental data. The best value of N_f has been found equal to 230 rpm, which is a reasonable value for the geometry of the contactor used in this work. Experience from previous work (Kirou et al., 1988) shows that at this agitation speed, even at very low phase flow rates, the column floods which means that a large number of drops cannot penetrate the critical layer between consecutive cells.

All frequency functions needed for the solution of Eq. 1 are now available. Before discussing calculated results and how they compare to experimental data, it is interesting to discuss some computational parameters. This subject is presented in the next section.

Discretization of the population balance equation

The population balance equation is discretized by volume so that all drop sizes produced by breakage and coalescence are represented in the discretization set. One difference between the batch stirred-cell contactor and the multistage column contactor is that the drop size distribution in the column contactor is much broader than in the batch system. In order to represent all sizes of a broad distribution in a volume discretization set, one has to use a large number of discrete sizes. The number of differential equations, N_{eq}, created by the discretization process increases linearly with the number of classes ($N_{eq} = 7 \times$ {number of classes}, for a seven-stage column), and the computational load increases in the same manner. In this study, the computational time has been substantially reduced by defining the maximum size to be the maximum experimental value rather than the feed-drop size. Hence, instead of using $d_{feed} = 2.7$ mm (average drop size introduced into the column) as the maximum diameter represented in the discretization set, we used the maximum measured drop size among all experimental conditions. A population balance equation resulting from the material balance is still written for the feed drop size. This equation includes an input term which represents the feed from the distributor and an output term due to breakage to smaller sizes. The set of classes is selected so that there is a sufficient number of classes (n_d) with size smaller than the critical diameter ($d < d_{cr}$). This number, n_d, has been determined to be larger than 5 in order that the effect of discretization on the results be minimal.

The system of integro-differential equations formed by discretization of Eq. 1 constitutes an initial value problem which is solved by the EPISODE routine (Byrne and Hindmarsh, 1976), an initial value solver package. The solution yields transient drop size distribution and holdup profiles. Comparisons of calculated and experimental values of these parameters are given in a subsequent section of this article. The experimental data are obtained from a multistage extraction column of pilot-plant scale which is described below.

Experimental Setup

Pilot plant

Experiments have been carried out on a multistage stirred-cell extraction column of pilot-plant scale which is described in detail by Kirou et al. (1988). The extractor diameter is 127 mm, and the height of each of its seven stages is 127 mm. The seven stages are formed by rings of 29% free area as compared to the column cross-sectional area. Mixing is provided by six-blade impellers of 63.5 mm diameter located at the center of each cell. The dispersed phase is introduced through a distributor located at the bottom of the extractor. The continuous phase is introduced at the top flowing to the bottom in a countercurrent mode with respect to the dispersed phase flow.

Chemical system

The chemical system used in this study is mutually equilibrated distilled water (continuous)-toluene (dispersed). For mass-transfer experiments, butyric acid has been used as the solute.

Measurement techniques

The holdup profile along the extractor is monitored by an ultrasonic technique which is described in detail by Bonnet and Tavlarides (1987), Tsouris et al. (1990a), and Yi and Tavlarides (1990). A photomicrographic technique (Kirou et al., 1988) is employed for steady-state drop size measurements.

Results and Discussion

Transient behavior of the holdup

The transient behavior of the holdup in the column contactor is studied in this section for step changes in the operating parameters. The average holdup calculated from the population balance model is compared to the experimental holdup at various operating conditions in Figure 5. The experimental average holdup is the average value of the measurements obtained from the seven cells of the column. In the experiment shown in Figure 5, the continuous-phase flow rate, Q_c, and the dispersed-phase flow rate, Q_d, are initially set to 0.54 L/min. At time $t = 0$, the agitation speed is set to 160 rpm. At time $t = 600$ s, the agitation speed is increased to 180 rpm to be reduced again to 160 rpm at 2,000 s. All three operating conditions changed at $t = 3{,}000$ s; Q_c is decreased to 0.42 L/min, Q_d is increased to 0.84 L/min, and the agitation speed is set to 170 rpm. Finally, at 4,000 s, the agitation speed is kept the same, while the flow rates of the two phases are interchanged, Q_c is set to 0.84 L/min and Q_d to 0.42 L/min. More experiments have been run (Tsouris, 1992) to study the transient behavior of the average holdup with respect to variations in the operating parameters (phase flow rates and agitation speed). In each of these experiments, a step disturbance was introduced in only one of the operating parameters. From the results, it can be concluded that the population balance model describes very well the transient behavior of the mean holdup in the multistage stirred-cell column contactor. The disadvantage of the model is that it predicts a weaker response of the holdup to variations of the continuous-phase flow rate than the experiments show. In general, the observed effect of the continuous-phase flow rate is very weak, suggesting that

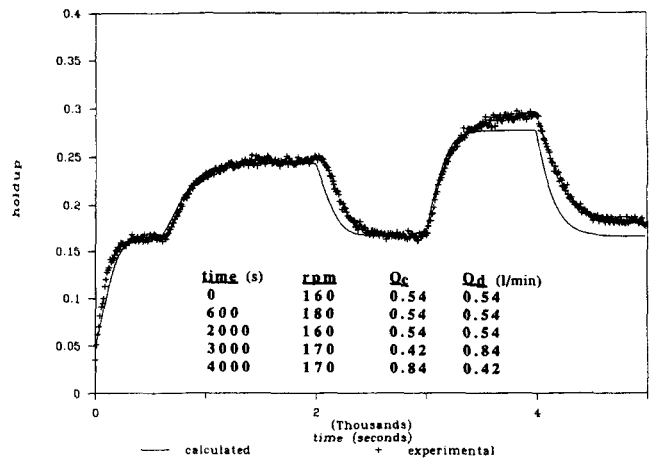

Figure 5. Comparison of calculated average transient holdup in a multistage column with experimental results.

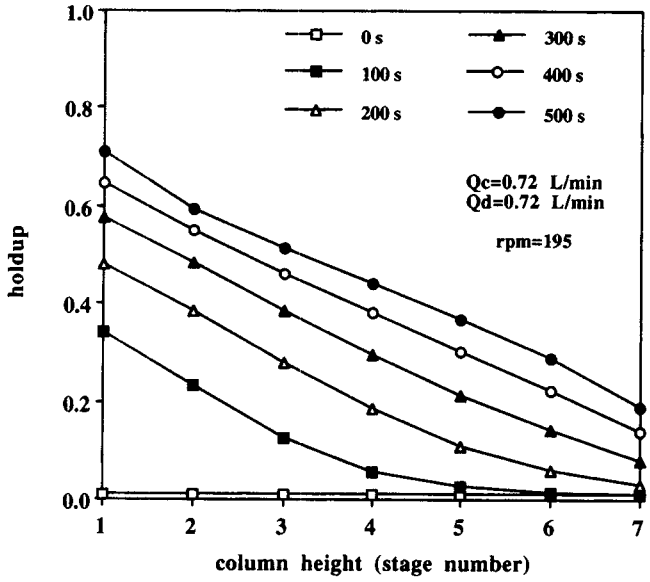

Figure 6. Calculated transient holdup profiles.

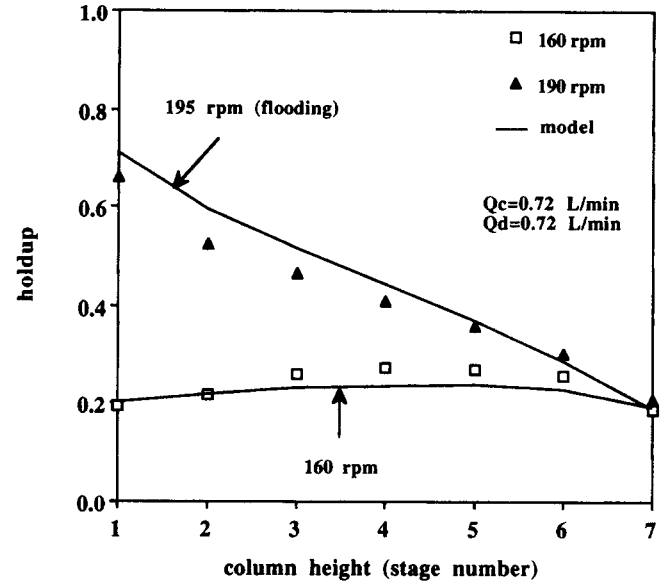

Figure 7a. Comparison of calculated and experimental holdup profiles.

in a control scheme, one should not use this operating condition as a manipulated variable for the control of the holdup.

The average holdup is an important parameter for the extraction process but not the only one. The drop size is equally important for the determination of the extent of the area of mass transfer between the two phases. Calculated results of drop size distribution and holdup profiles are compared with experimental data in the next section.

Steady-state drop size and holdup profiles

Profiles of drop size distribution and holdup along the column contactor present a stringent test for the population balance model. Calculated results for holdup and d_{32} are compared in this section with experimental data obtained in previous studies (Kirou et al., 1988; Tsouris et al., 1990b).

The holdup profile at flooding conditions has been reported (Kirou et al., 1988) to have a maximum value in the first stage. Calculated holdup profiles from the population balance model at flooding conditions are shown in Figure 6. In these results, the selected initial condition at $t=0$ gives approximately 1% holdup. As time evolves, the holdup profile increases showing a maximum in the first stage. This behavior is similar to what is observed experimentally. It should be mentioned here that, once the holdup maximum in the first stage reaches approximately 70%, the holdup values become unstable due to the fact that the algorithm does not accommodate drop rejection from stage 1 with the continuous-phase exit stream. The lack of this term results in holdup values greater than 1, which are unacceptable, and then oscillations are observed in all values of the holdup profile. The profile at $t=500$ s is also shown in Figure 7a, where calculated and experimental results are compared at different values of agitated speed. This comparison shows the differences between normal and flooding holdup profiles. In general, the maximum in the holdup profile moves from the upper cells towards lower cells as the agitation speed increases. The error in the mean holdup is of order 15%. The same magnitude of error is observed in the d_{32} profile shown

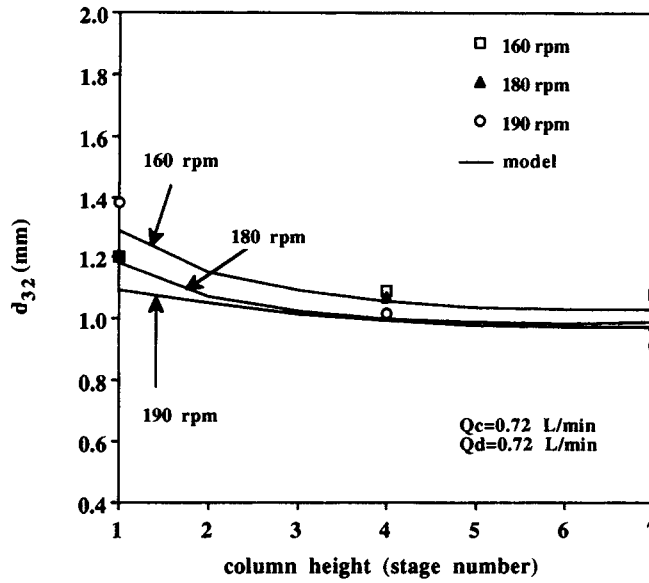

Figure 7b. Comparison of calculated and experimental Sauter mean diameter.

in Figure 7b. In the lower cells where the dispersed phase is introduced, the drop size is larger. As the drops travel upwards in the column due to buoyancy, drop breakage occurs and the drop size decreases. The higher the agitation speed the more intense the breakage. However, the holdup increases also with the agitation speed causing a different effect on the drop size. The effect of the holdup is quantitatively introduced in the energy dissipation as a turbulence damping factor (see Tsouris and Tavlarides, 1994). During transient behavior, the holdup changes with time and, therefore, the values of energy dissipation, breakage, coalescence, and exit are updated during the calculations.

More comparisons of calculated and experimental results of

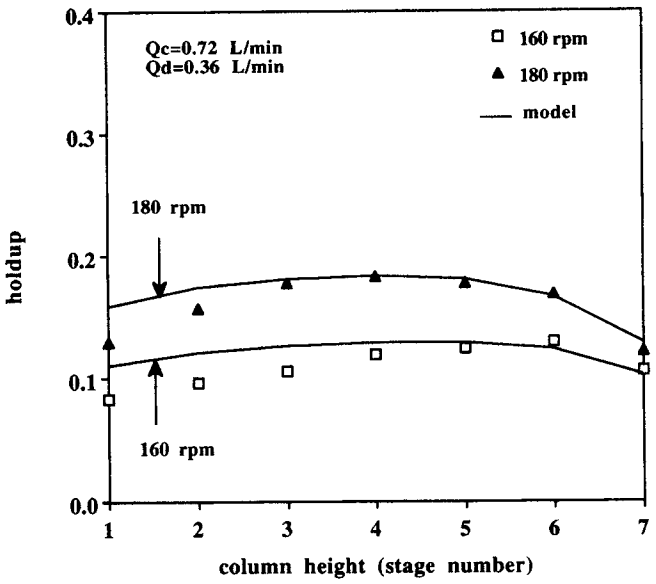

Figure 8a. Comparison of calculated and experimental holdup profile.

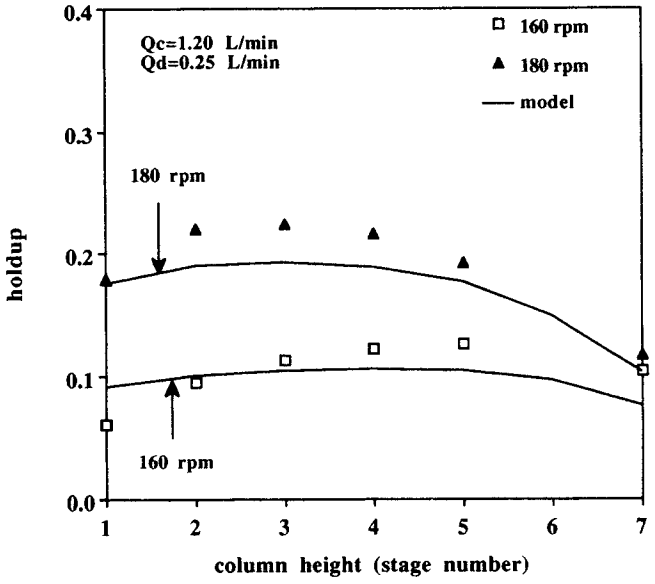

Figure 9a. Comparison of calculated and experimental holdup profiles.

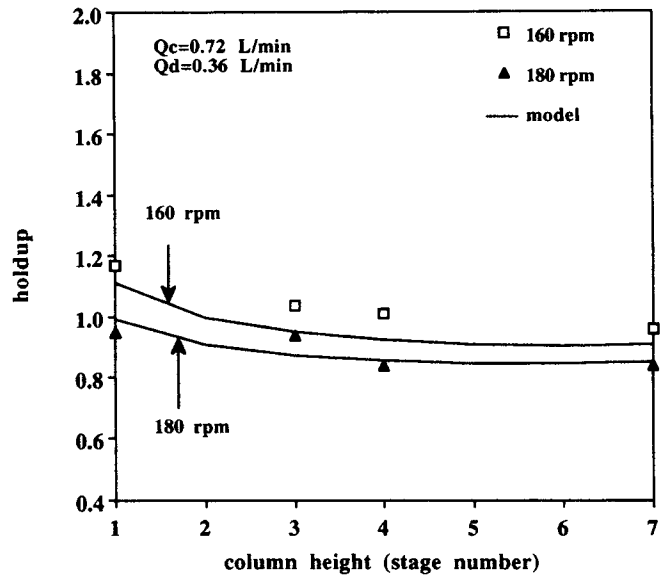

Figure 8b. Comparison of calculated and experimental Sauter mean diameter.

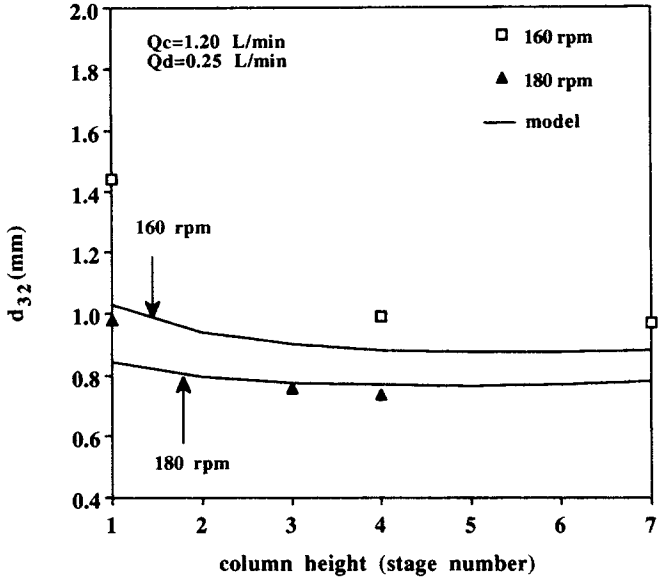

Figure 9b. Comparison of calculated and experimental Sauter mean diameter.

holdup and d_{32} profiles are given in Figures 8a, 8b, 9a, and 9b at various operating conditions. Furthermore, the steady-state drop size distribution of the fourth cell is compared in Figure 10 for two levels of agitation speed in the form of cumulative volume fraction. The model predictions tally quite well at the higher rpm of 180 but do not match well with the experimental results for large drop sizes at 160 rpm. A relative error of approximately 15% is observed between the predictions and the calculated results at the lower agitation speed, whereas a better agreement is observed for the higher agitation speed.

Effect of Mass Transfer

Extraction experiments (Tsouris, 1992) revealed that mass transfer has a significant effect on the drop behavior in liquid dispersions. In the case of solute transfer from the continuous phase to the drops, smaller drop sizes are observed due to higher breakage rates. The smaller drops have longer residence times and, therefore, the holdup increases. In the other case of mass transfer, from the drops to the continuous phase, the coalescence rate is enhanced creating larger drops and lower holdup.

The behavior of the mass-transfer system from the continuous-phase to the drops is explained by the variations in the interfacial tension between the two phases. The interfacial tension of the water-butyric acid-toluene system is measured at equilibrium for various concentrations of butyric acid, and results are shown in Table 1. For the calculation of the holdup, the interfacial tension, σ, is estimated by assuming equilibrium

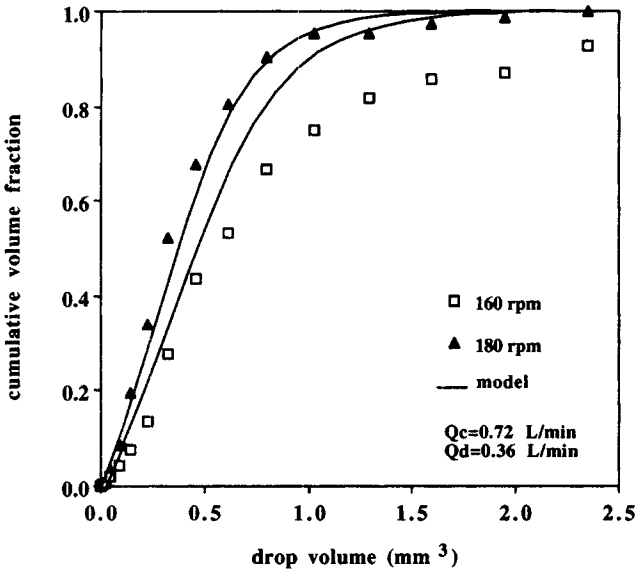

Figure 10. Comparison of calculated and experimental cumulative volume fraction in the fourth stage of the column at steady state.

between the two phases and using Table 1 to read the interfacial tension at the aqueous phase concentration.

When two drops are in contact during mass transfer from the drops to the continuous phase, the concentration in the liquid film between the drops is equilibrated rapidly with the drop concentration. This phenomenon creates interfacial tension gradients which in turn cause interfacial flow. The enhanced mobility of the interface, due to interfacial flow, squeezes the continuous-phase film between the drops rapidly and, consequently, the drop coalescence rate is enhanced. Therefore, even though breakage is more intense than the solute-free system due to lower interfacial tension, the coalescence rate dominates and forces the drop size to increase until the two drop-rate processes become equivalent. Drops as large as ~1-2 cm were observed experimentally (see Tsouris and Tavlarides, 1993). These drops are not spherical; they do not follow the continuous-phase flow patterns, and, in general, the limits of applicability of the breakage, coalescence, and exit models have been exceeded. Computed results in this case are not reliable. Figure 11 shows the experimental holdup profiles for all modes of operation and the calculated results for the cases of (1) no mass transfer and (2) mass transfer from the continuous phase to the drops.

Simulation of Process Control

An experimental study of the control of the extraction column has been reported earlier (Tsouris and Tavlarides, 1991). In that study, the control of the dispersed-phase volume fraction was demonstrated by modeling the process with a first-order with dead time transfer function and the Dahlin algorithm as the controller. As a first step towards "model based predictive control," the population balance model described herein is employed to simulate the extraction column. The previously developed controller is applied for servo and regulatory control for both the simulated column and the experimental apparatus for comparisons. The controller equation obtained from the Dahlin algorithm is given by:

Table 1. Interfacial Tension vs. Concentration of Butyric Acid at Equilibrium

Concentration of Butyric Acid, wt. %		Interfacial Tension
In Toluene	In Water	dyne/cm
0	0	27.0
0.032	0.016	20.7
0.068	0.026	16.4
0.114	0.035	12.4
0.155	0.042	12.3

$$G_c = \frac{\tau}{K(\lambda+\theta)}\left(1+\frac{1}{\tau S}\right). \tag{31}$$

Here, τ is the open-loop time constant, K is the gain of the process, θ is the dead time, λ is the closed-loop time constant or the Dahlin parameter, and S is the Laplace variable. The simulation of this controller, by using the population balance model, is shown here for both servo and regulatory control, and results are compared with the experimental response. Figure 12a shows the simulation of servo control for λ given by the following relation (Bray et al., 1990):

$$\log \lambda = -0.522 + 0.918 \log \tau \tag{32}$$

The upper curve in Figure 12a shows the agitation speed which is the manipulated variable, whereas the lower curve shows the control variable, ϕ. The simulated response is very similar to the experimental response shown in Figure 12b. The regulatory control is shown in Figures 13a and 13b for disturbances, first, in the dispersed phase flow rate and, second, in the continuous-phase flow rate. In this experiment, the value of λ is 0.75τ. The simulated response (Figure 13a) is shown to

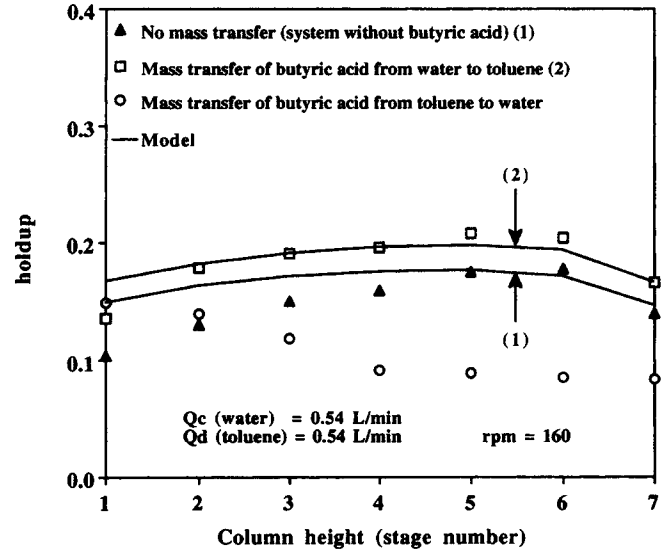

Figure 11. Effect of mass transfer of solute on the holdup profile.

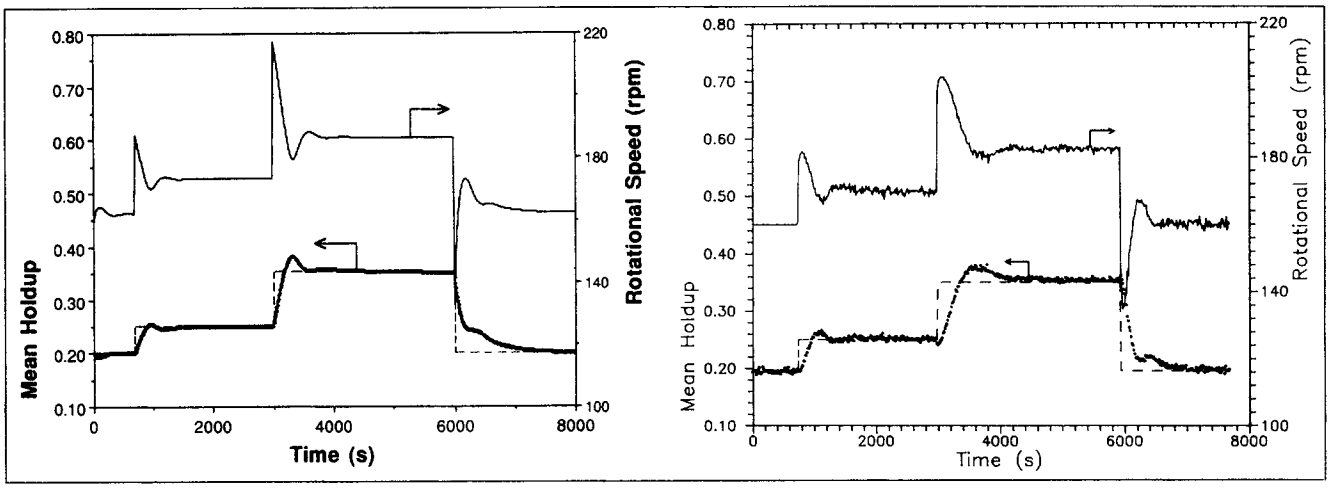

Figure 12. Servo control of the holdup: (a) simulation; (b) experimental.

Flow rates: $Q_d = 0.54$ L/min, $Q_c = 0.54$ L/min; set point: $\phi_{sp} = 0.20 - 0.25 - 0.35 - 0.20$.

be faster than the experimental, but the difference in the maximum deviation for both disturbances is only two percentage units of the holdup.

The comparison between the simulation and the real process leads to the conclusion that the population balance equation represents very well the process for physically equilibrated systems. These results suggest that the pbe models can be used for model based control of extraction columns for physically equilibrated systems and can be extended to cases with mass transfer.

Conclusions

In summary, the population balance model for a multistage stirred-cell extraction column is solved numerically, providing information regarding the hydrodynamic behavior of the column. Drop rate functions of breakage and coalescence are used as developed for a stirred-tank contactor. A drop exit frequency is developed to link the population balance equations of consecutive cells. The model is found to describe satisfactorily both the transient behavior of holdup and the steady-state behavior of holdup and d_{32} profiles. The qualitative holdup behavior at flooding conditions is also predicted well. There are, however, some discrepancies between calculations and experimental data which are due to inadequacies of the drop breakage, coalescence, and exit models. These functions need further improvement to enhance the predictive capabilities of the model.

The effect of mass transfer on the hydrodynamic behavior of the column is briefly discussed. Although the model trends are in the right direction, a complete description of the mass-transfer behavior on the column hydrodynamics should include a more fundamental approach for the effect of mass transfer on the drop coalescence and breakage frequencies. This de-

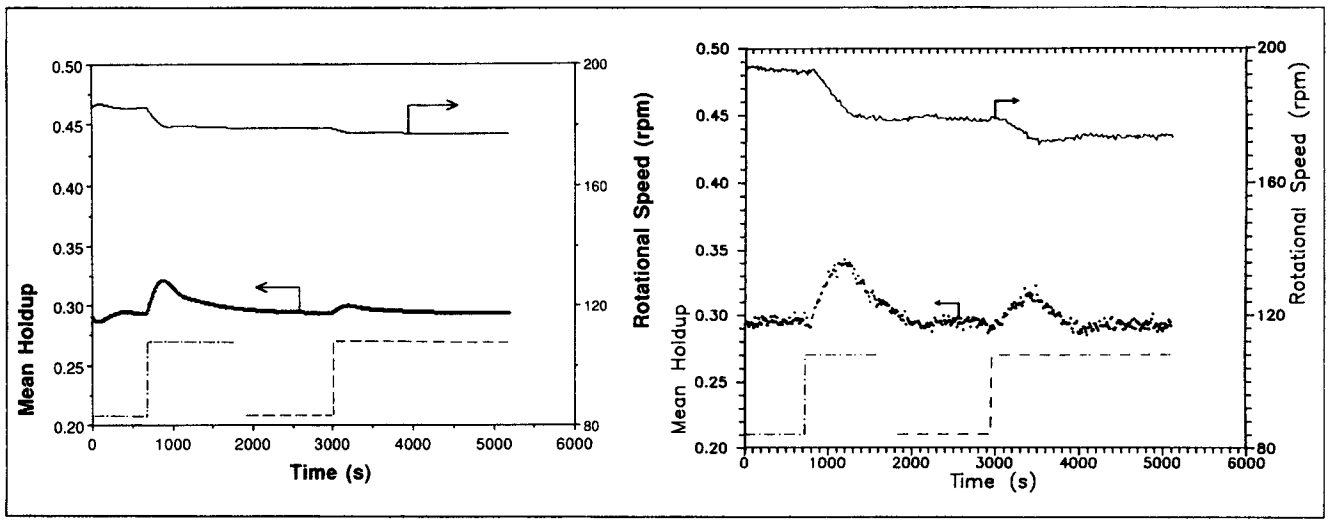

Figure 13. Regulatory control of the holdup: (a) simulation; (b) experimental.

Flow rates: $Q_d = 0.54$ L/min ~ 700 s $\rightarrow$ 0.72 L/min; $Q_c = 0.54$ L/min $\sim 3{,}000$ s $\rightarrow$ 0.72 L/min; set point: $\phi_{sp} = 0.30$.

velopment, however, is beyond the scope of this work which aims to demonstrate the utilization of the population balance equation for modeling extraction columns. Finally, the population-balance-equation model can be employed for model-based process control under the constraints of the applicability of these models.

Acknowledgment

The authors gratefully acknowledge the National Science Foundation through grant CTS-9017138 for the support of this work. We also thank Ms. Nicole Jones for carefully preparing both manuscripts.

Notation

B = birth terms
d = drop diameter, m
d_{cr} = critical drop diameter below which drops do not break, m
d_{feed} = feed drop diameter, m
D = death terms
D_i = impeller diameter, m
D_T = tank diameter, m
F_{exp} = frequency of exposure, s^{-1}
$g(v)$ = breakage of frequency, s^{-1}
G_c = controller transfer function
$h(d_i, d_j)$ = collision frequency, s^{-1}
$h(v_i, v_j)$ = collision frequency, s^{-1}
H = tank height, m
K = process gain
n = number density of particles, m^{-1}
N = agitation speed, s^{-1}
N_{eq} = number of equations
N_f = agitation speed defined by Eq. 16, s
P_{exit} = exit probability
P_{loop} = probability for a drop to be in the circulation loop
Q_c = continuous-phase flow rate, $m^3 \cdot s^{-1}$
r_c = radius defined by Eq. 16, m
r_f = radius of free area between consecutive stages, m
r' = radius shown in Figure 4, m
rpm = agitation speed, min^{-1}
rps = agitation speed, s^{-1}
S = Laplace variable
t_e = exit time, s
t_p = penetration time, s
u = velocity, $m \cdot s^{-1}$
u_c = continuous-phase velocity component, $m \cdot s^{-1}$
$u(d)$ = terminal velocity, $m \cdot s^{-1}$
$u_d(d)$ = drop velocity in a stagnant medium, $m \cdot s^{-1}$
u_{tip} = impeller tip velocity, $m \cdot s^{-1}$
u_z = fluctuating velocity component, $m \cdot s^{-1}$
U_c = continuous phase velocity, $m \cdot s^{-1}$
U_{max} = maximum velocity, $m \cdot s^{-1}$
v = volume, m^3
V_{loop} = volume of the circulation loop, m^3
V_T = volume of a single cell of the column
z_e = exit frequency, s^{-1}

Greek letters

$\beta(v_i, v_j)$ = probability density of drops v_j produced by breakage of drops v_i
δ = critical layer, m
$\Delta\rho$ = density difference, $kg \cdot cm^{-3}$
ϵ = energy dissipation, $m^2 \cdot s^{-3}$
θ = dead time of the process, s
λ = closed-loop time constant (Dahlin parameter), s
$\lambda(d_i, d_j)$ = coalescence efficiency
$\lambda(v_i, v_j)$ = coalescence efficiency
μ = viscosity, $kg \cdot m^{-1} \cdot s^{-1}$
μ^* = mean value in Eq. 26
ν = number of drops produced from a drop breakup
ν = kinematic viscosity, $m^2 \cdot s^{-1}$
ρ = density, $kg \cdot m^{-3}$
σ = interfacial tension, $N \cdot m^{-1}$
σ^* = standard deviation in Eq. 26
τ = open-loop time constant, s
ϕ = holdup

Literature Cited

Bapat, P. M., and L. L. Tavlarides, "Mass Transfer in a Liquid-Liquid Continuous Flow Stirred Tank Reactor," *AIChE J.*, **31**, 659 (1985).

Bapat, P. M., L. L. Tavlarides, and G. W. Smith, "Monte Carlo Simulation of Mass Transfer in Liquid-Liquid Dispersions," *Chem. Eng. Sci.*, **38**, 2003 (1983).

Bonnet, J. C., and L. L. Tavlarides, "Ultrasonic Technique for Dispersed-Phase Holdup Measurements," *I&EC Res.*, **26**, 811 (1987).

Bray, S., M. Medina, and C. A. Smith, "A Method for the Determination of Dahlin's Algorithm Parameters," *I&EC Res.*, **29**, 924 (1990).

Byrne, G. D., and A. C. Hindmarsh, "EPISODE: An Experimental Package for the Integration of Systems of Ordinary Differential Equations," UCID-30132, Computer Documentation, Lawrence Livermore Laboratory, Univ. of California, Berkeley, CA (1976).

Casamatta, G., and A. Vogelpohl, "Modelling of Fluid Dynamics and Mass Transfer in Extraction Columns," *Germ. Chem. Eng.*, **8**, 96 (1985).

Cruz-Pinto, J. J. C., and W. J. Korchinsky, "Drop Breakage in Countercurrent Flow Liquid-Liquid Extraction Columns," *Chem. Eng. Sci.*, **36**, 687 (1981).

Gourdon, C., and G. Casamatta, "Influence of Mass Transfer Direction on the Operation of a Pulsed Sieve-Plate Pilot Column," *Chem. Eng. Sci.*, **46**, 2799 (1991).

Guimaraes, M. M. L., J. J. C. Cruz-Pinto, P. F. R. Requeiras, and C. M. N. Madureira, *The Simulation of Interacting Liquid-Liquid Dispersions—A New Algorithm and Its Potentiality*, Int. Solvent Extraction Conf. Proc., Elsevier, Essex, England, p. 1241 (1990).

Holmes, D. B., R. M. Vonken, and J. A. Dekker, "Fluid Flow in Turbine-Stirred, Baffled Tanks I: Circulation Time," *Chem. Eng. Sci.*, **19**, 201 (1964).

Hsia, M. A., and L. L. Tavlarides, "A Simulation Model for Homogeneous Dispersions in Stirred Tanks," *Chem. Eng. J.*, **20**, 225 (1980).

Hsia, M. A., and L. L. Tavlarides, "Simulation and Analysis of Drop Breakage, Coalescence, and Micromixing in Liquid-Liquid Stirred Tanks," *Chem. Eng. J.*, **26**, 189 (1983).

Hulburt, H. M., and S. Katz, "Some Problems in Particle Technology. A Statistical Mechanical Formulation," *Chem. Eng. Sci.*, **19**, 555 (1964).

Jiricny, V., M. Kratky, and J. Prochazka, "Counter-Current Flow of Dispersed and Continuous Phase-I: Discrete Polydispersed Model," *Chem. Eng. Sci.*, **34**, 1141 (1979).

Jiricny, V., M. Kratky, and J. Prochazka, "Counter-Current Flow of Dispersed and Continuous Phase-I: Simulation of Holdup and Particle Size Distribution Profiles," *Chem. Eng. Sci.*, **34**, 1151 (1979).

Ju, S. Y., T. M. Mulvahill, and R. W. Pike, "Three-Dimensional Turbulent Flow in Agitated Vessels with a Nonisotropic Turbulent Model," *Can. J. Chem. Eng.*, **68**, 3 (1990).

Kirou, V. I., "Stochastic Simulation of Dispersed Phase Holdup and Drop Size Distribution in a Mixer Column Contactor," PhD Dissertation, Syracuse University, Syracuse, NY (1990).

Kirou, V. I., and L. L. Tavlarides, "Stochastic Simulation of Holdup and Drop Size Distribution Profiles in Column Extractors," submitted for publication in *Chem. Eng. Sci.* (1994).

Kirou, V. I., L. L. Tavlarides, J. C. Bonnet, and C. Tsouris, "Flooding, Holdup, and Drop-Size Measurements in a Multistage Column Extractor," *AIChE J.*, **34**, 283 (1988).

Klee, A. J., and R. E. Treybal, "Rate of Rise and Fall of Liquid Drops," *AIChE J.*, **2**, 444 (1956).

Laso, M., L. Steiner, and S. Hartland, "Modeling of Axial Hold-up and Drop Size Distribution Profiles in a Liquid-Liquid Extraction Column," paper D7.8, CHISA 84, Prague, Czechoslovakia (Sept. 3-7, 1984).

Ramkrishna, D., "The Status of Population Balances," *Rev. Chem. Eng.*, **3**, 49 (1985).
Randolph, A. D., and M. A. Larson, *Theory of Particulate Processes. Analysis and Techniques of Continuous Crystallization*, Academic Press, New York (1971).
Ross, S. L., "Measurements and Models of the Dispersed Phase Mixing Process," PhD Dissertation, The University of Michigan, Ann Arbor, MI (1971).
Ross, S. M., *Introduction to Probability Models*, 2nd ed., Academic Press, NY (1980).
Schwartzberg, H. G., and R. E. Treybal, "Fluid Particle Motion in Turbulent Stirred Tanks," *Ind. Eng. Chem. Fundam.*, **7**, 1 (1968).
Shah, B. H., D. Kamkrishna, and J. D. Borwanker, "Simulation of Particulate Systems using the Concept of the Interval of Quiescence," *AIChE J.*, **23**, 897 (1977).
Sovova, H., "A Model of Dispersion Hydrodynamics in a Vibrating Plate Contactor," *Chem. Eng. Sci.*, **38**, 1863 (1983).
Spielman, L. A., and O. Levenspiel, "A Monte Carlo Treatment for Reacting and Coalescing Dispersed Phase Systems," *Chem. Eng. Sci.*, **20**, 247 (1965).
Tsouris, C., and L. L. Tavlarides, "Comments on Model for Holdup Measurements in Liquid Dispersions Using an Ultrasonic Technique," *I&EC Res.*, **29**, 2170 (1990).
Tsouris, C., L. L. Tavlarides, and J. C. Bonnet, "Application of the Ultrasonic Technique for Real-Time Holdup Monitoring for the Control of Extraction Columns," *Chem. Eng. Sci.*, **45**, 3055 (1990a).
Tsouris, C., R. Ferreira, and L. L. Tavlarides, "Characterization of Hydrodynamic Parameters in a Multistage Column Contactor," *Can. J. Chem. Eng.*, **68**, 913 (1990b).
Tsouris, C., and L. L. Tavlarides, "Control of Dispersed-Phase Volume Fraction in Multistage Extraction Columns," *Chem. Eng. Sci.*, **46**, 2857 (1991).
Tsouris, C., and L. L. Tavlarides, "Mass Transfer Effects on Droplet Phenomena and Extraction Column Hydrodynamics Revisited," *Chem. Eng. Sci.*, **48**, 1503 (1993).
Tsouris, C., and L. L. Tavlarides, "Breakage and Coalescence Models for Drops in Turbulent Dispersions," *AIChE J.*, **40**, 395 (1994).
Tsouris, C., "Modeling and Control of Extraction Columns," PhD Thesis, Syracuse University, Syracuse, NY (1992).
Yi, J., and L. L. Tavlarides, "A Model for Holdup Measurements in Liquid Dispersions Using the Ultrasonic Technique," *I&EC Res.*, **29**, 475 (1990).
Zeitlin, M. A., and L. L. Tavlarides, "Fluid-Fluid Interactions and Hydrodynamics in Agitated Dispersions: A Simulation Model," *Can. J. Chem. Eng.*, **50**, 207 (1972).

Manuscript received July 13, 1992, and revision received July 6, 1993.